Eur. Phys. J. Plus (2020) 135:62
https://doi.org/10.1140/epjp/s13360-020-00103-6

THE EUROPEAN PHYSICAL JOURNAL PLUS

Regular Article

Study of multi-quasiparticle energy bands in neutron-deficient ^{117,119,121}Cs

Rawan Kumar[1], **Shivali Sharma**[2], **Rani Devi**[2,a]

[1] Department of Higher Education, Government of Jammu and Kashmir, Jammu and Kashmir, India
[2] Department of Physics, University of Jammu, Jammu, Jammu and Kashmir 180006, India

Received: 3 May 2019 / Accepted: 3 January 2020

Abstract The projected shell model is employed to interpret multi-quasiparticle energy bands in odd-mass neutron-deficient $^{117-121}$Cs isotopes. The experimentally known energy bands and their configurations are reproduced well by employing this approach. The analysis of theoretical results predicts the low-lying spin states to arise from the single quasiparticle band albeit the high-spin states are seen to arise from the superposition of three quasiparticle bands. In addition, the experimentally known signature partner bands and band head energies are also predicted in these isotopes which can serve as a clue for planning new experiments.

1 Introduction

The overview of experimental literature provides the evidence that neutron-deficient cesium isotopes are deformed and show intriguing collective behavior [1–5]. In these isotopes, it is interesting to study the variation in collectivity and nuclear shapes with change in spin and neutron number. Smith et al. [6] have performed high-spin spectroscopy of ^{117}Cs using Gammasphere array and extended the previously observed negative parity band [7] to high spins. They have observed two additional bands that were tentatively assigned to be based on protons in the [404]9/2$^+$ and [422]3/2$^+$ orbitals. They observed alignments of pairs of $1h_{11/2}$ neutrons and protons in all the bands. The first $(h_{11/2})^2$ neutron alignments occur at frequencies 0.40, 0.38 and 0.40 MeV/$\hbar$ in bands 1, 2, and 3, respectively. Liden et al. [1] have extended $1h_{11/2}$ unique parity band of ^{119}Cs from $I^\pi = 27/2^-$ [8] up to $I^\pi = 35/2^-$ and $g_{9/2}$ band structure up to $I^\pi = 25/2^+$ level.

High-spin structures of ^{121}Cs have been previously studied by Garg et al. [8] and Liden et al. [1]. Moon et al. [9] have extended the previously known positive and negative parity bands to high spins. They have established three rotational bands built on the negative parity $1h_{11/2}$ orbital. They have also identified an unfavored and a favored rotational band. In recent nuclear data sheets, two positive parity and four negative parity bands are observed for this nucleus [10].

Earlier some theoretical attempts [1, 2, 6, 8] have been employed to study the high-spin states in $^{117-121}$Cs isotopes. For example, Smith et al. [6] have performed Cranked Woods–Saxon (CWS) calculations for ^{117}Cs and compared the alignment of $1h_{11/2}$ neutrons and protons. In case of negative parity Band 1, only one signature partner band is observed.

[a] e-mail: rani_rakwal@yahoo.co.in

Published online: 13 January 2020

This band is based on $1h_{11/2}$ orbital. The observed upbend in this band at 0.45 MeV/$\hbar$ is attributed to the alignment of the first pair of $1h_{11/2}$ neutrons. In case of positive parity Band 2 also only one signature partner of the band is observed. They predicted that two candidate Nilsson orbitals near the Fermi surface would be $\pi(g_{7/2}/d_{5/2})[422]3/2^+$ and $[420]1/2^+$. Total-Routhian-surface (TRS) calculations predict that $[422]3/2^+$ band lies slightly lower in energy than the $[420]1/2^+$ band and thus it is likely that the band head of Band 2 is the $3/2^+$ state of the $[422]3/2^+$ band. In case of Band 3, they have assigned $\pi(g_{9/2})[404]9/2^+$ configuration. They have suggested that the alignment frequencies can be qualitatively explained only if a n–p interaction is taken into account. Liden et al. [1] have carried out TRS calculations using a deformed Woods–Saxon potential and the Strutinsky shell-correction formalism with a monopole pairing interaction. In case of ^{119}Cs, for $[404]9/2^+$ band the $1h_{11/2}$ proton alignment is predicted to occur at $\hbar\omega = 0.36$ MeV. In the $[550]1/2^-$ band, they have predicted $1h_{11/2}$ neutron crossing frequency at $\hbar\omega = 0.38$ MeV, which is lower than the experimental value. In case of ^{121}Cs, they predicted that minimum of the $[550]1/2^-$ configuration is pure in the TRS calculations, since all the states of negative parity band originate from the $1h_{11/2}$ shell with no mixing of other states. The deformation of this structure was calculated to remain stable at $\beta_2 = 0.25$, $\gamma = 5°$ up to the first band crossing. They have predicted crossing frequency for the $[422]3/2^+$ configuration to be $\hbar\omega_c = 0.42$ MeV and for the $[404]9/2^+$ configuration to be $\hbar\omega_c = 0.37$ MeV. Due to complexity of $[[550]1/2^- \otimes [422]3/2^+ \otimes [404]9/2^+]$ band structure, no quasiparticle calculations were performed. They were able to reproduce relative experimental band-head deformation theoretically. Garg et al. [8] have performed particle-plus-rotor and particle-plus-vibrator model calculations for $^{119-125}$Cs and found that agreement between calculated energy levels and experimental values worsen for high-spin states. In mass region around $A = 120$, cranked shell model (CSM) calculations suggest that the first band crossing is due to the rotational alignment of a pair of $1h_{11/2}$ neutrons at $\hbar\omega = 0.40$ MeV. The shape driving force of the aligned pair depends on the position of the neutron Fermi surface within the $1h_{11/2}$ subshell; neutrons in the upper midshell favor a collective oblate shape, while those in the lower midshell favor collective prolate shapes [2].

In the present work, the projected shell model (PSM) is applied to investigate the band structures of neutron-deficient odd proton Cs isotopes. In this model, one can include a large configuration space by taking deformed basis states. The study of variety of nuclei [11–26] has already been undertaken by employing PSM and satisfactory agreement has been obtained with the available experimental data on yrast bands. To study all the multi-quasi particle bands by taking same set of parameters is a demanding job for shell model like calculations. In this study, it is demonstrated that all the observed experimental bands in neutron-deficient ^{117,119,121}Cs nuclei can be reproduced by taking the Nilsson parameter set that is already employed for the study of even–even nuclei in A ~ 120 mass region [19–22] in the previous works.

The organization of the present paper is as: Sect. 2 presents a brief description of PSM theory followed by results and discussion in Sect. 3. Section 3 is comprised of three subsections, describing the calculated energy level scheme of each of three Cs isotopes in detail. The signature splitting phenomenon is presented in Sect. 4. Finally, the paper ends with summary in Sect. 5.

2 Outline of projected shell model

The detailed description of PSM theory is presented by the authors of Refs. [27, 28] in their review articles. The outline of the model is presented here for completion. To understand

Table 1 Deformation parameters for $^{117-121}$Cs

Nucleus	ε_2	ε_4
^{117}Cs	0.257	− 0.035
^{119}Cs	0.250	− 0.035
^{121}Cs	0.257	− 0.045

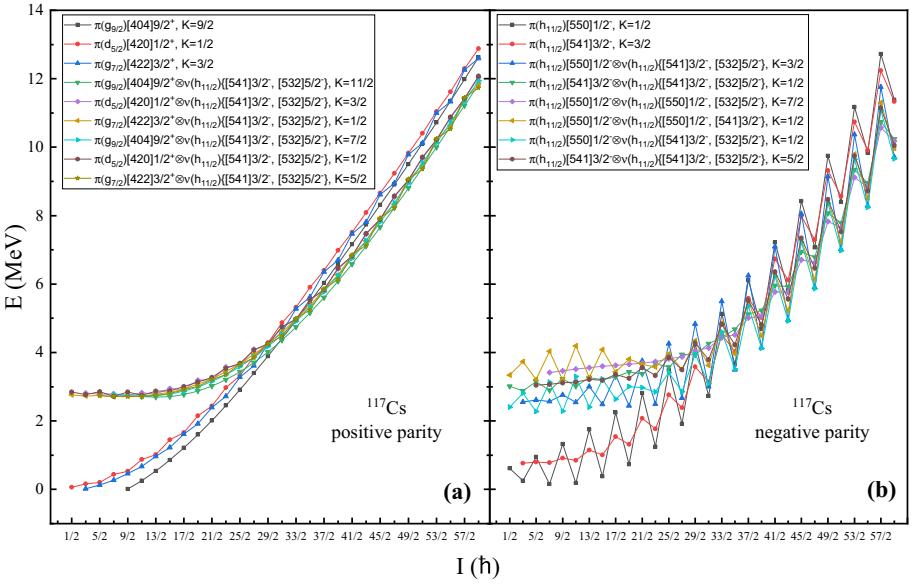

Fig. 1 Band diagrams for several lowest lying one-quasiproton and the corresponding 3-qp (one-quasiproton + neutron pair) bands in ^{117}Cs. Bands are characterized by different curve types as shown in Fig. boxes. **a** Left: positive parity **b** Right: positive parity bands

the evolution of collectivity up to high-spin states of positive and negative parity bands of $^{117-121}$Cs, the PSM is employed. Previously, the systematics of some even–even nuclei in the mass region $A \sim 120$ [19–22] have been studied by using the same model. A systematic study of yrast bands in odd proton nuclei in the $A \sim 120$ mass region is also performed by Ibáñez-Sandoval et al. [12]. The starting point of PSM is the deformed Nilsson model [29], the diagonalization of which gives the deformed single-particle basis. In the next step, the pairing correlations are added by a BCS calculation and the Nilsson-BCS basis is constructed by taking an energy window around the Fermi surface. The technique of angular momentum projection [30] is employed to restore the broken rotational symmetry. The next step in the PSM calculation is the diagonalization of the two-body shell model Hamiltonian in the projected space. In the last step of the PSM calculation, the various configurations are mixed as is done in the usual shell model calculation, but the configuration space will be taken as small, as compared to shell model.

The superposition of projected multi-quasiparticle states forms the PSM wave function which is given by:

$$\left|\psi_M^I\right\rangle = \sum_{\kappa K} f_{\kappa K}^I P_{MK}^I |\phi_\kappa\rangle, \tag{1}$$

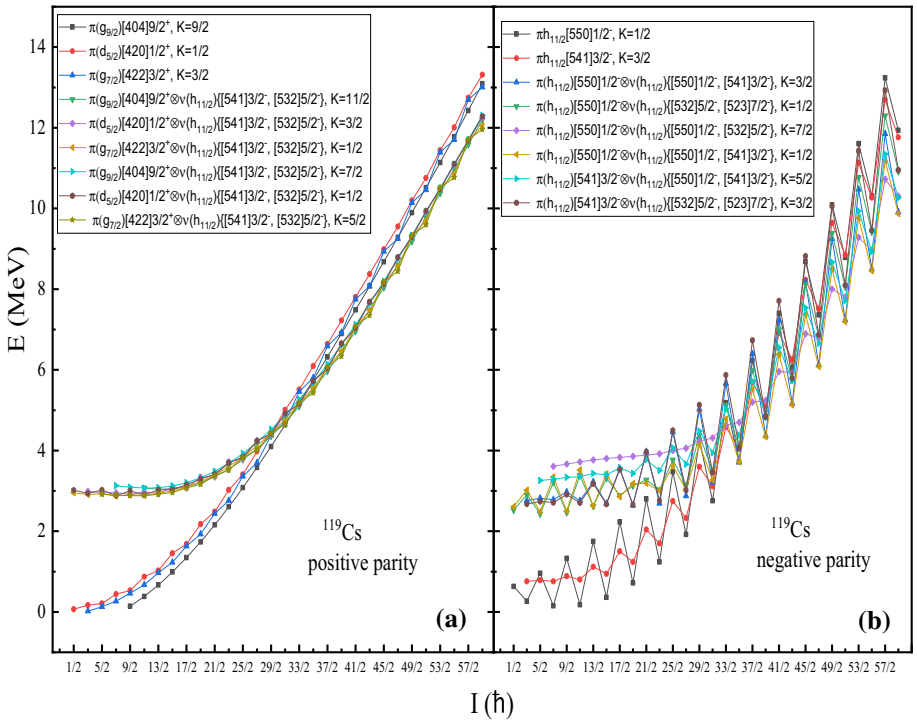

Fig. 2 Band diagrams for several lowest lying one-quasiproton and the corresponding 3-qp (one- quasiproton + neutron pair) bands in ^{119}Cs. Bands are characterized by different curve types as shown in Fig. boxes. **a** Left: positive parity **b** Right: negative parity bands

where quasiparticle (qp) basis is denoted by $|\phi_\kappa\rangle$, $f^I_{\kappa K}$ are the weight factors of the basis states which are obtained by the diagonalization of shell model Hamiltonian. The angular momentum projection operator P^I_{MK} projects out from the intrinsic configuration $|\phi_\kappa\rangle$ good angular momentum states.

In PSM calculations, usually three harmonic oscillator shells are taken for each type of nucleon, therefore in the present study, three major oscillator shells which are taken are $N = 3$, 4 and 5 for each type of nucleons. The quasiparticle states near the Fermi energy in $N = 4(5)$ major shell for protons (neutrons) are selected for constructing the configuration space for the positive parity bands. For the negative parity bands, the configuration space is made by choosing the quasiparticle states close to Fermi energy in $N = 5$ shell.

The quasiparticle configuration space $|\phi_\kappa\rangle$ for the study of odd Z Cs nuclei is taken as

$$|\phi_\kappa\rangle = \left\{\alpha^\dagger_{\pi_i}|0\rangle, \alpha^\dagger_{\pi_i}\alpha^\dagger_{\upsilon_j}\alpha^\dagger_{\upsilon_k}|0\rangle\right\} \tag{2}$$

where $\alpha^\dagger$ is the creation operator for a qp and the index $\upsilon(\pi)$ denotes neutron (proton) Nilsson quantum numbers which run over the orbitals close to the Fermi levels. In the case of odd Z nuclei, the ground state band is a 1-qp proton band and as one moves to higher spins, 3-qp ($1\pi \otimes 2\nu$) bands cross the ground state bands and contribute to the yrast band. Therefore, the model space of Eq. (2) is enough for studying the high-spin properties of odd Z nuclei.

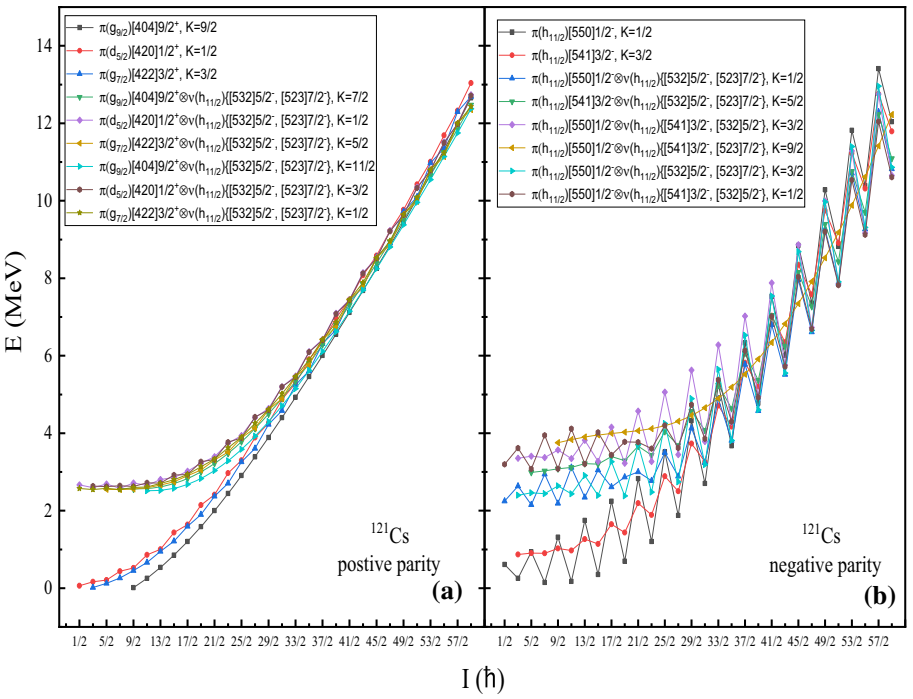

Fig. 3 Band diagrams for several lowest lying one-quasiproton and the corresponding 3-qp (one-quasiproton + neutron pair) bands in ^{121}Cs. Bands are characterized by different curve types as shown in Fig. boxes. **a** Left: positive parity **b** Right: negative parity bands

The Hamiltonian that is employed in the PSM calculations consists of quadrupole–quadrupole interaction, monopole and quadrupole pairing forces [27, 28].

$$\hat{H} = \hat{H}_0 - \frac{\chi}{2}\sum_{\mu}\hat{Q}^{\dagger}_{2\mu}\hat{Q}_{2\mu} - G_M\hat{P}^{\dagger}\hat{P} - G_Q\sum_{\mu}\hat{P}^{\dagger}_{2\mu}\hat{P}_{2\mu} \tag{3}$$

In Eq. (3), the spherical single-particle Hamiltonian which can take a proper spin–orbit force is represented by $\hat{H}_0$. The relation for the monopole pairing strength G_{M} is taken as $G_{\mathrm{M}\nu} = [G_1 - G_2(N-Z)/A]/A$ for neutrons and $G_{\mathrm{M}\pi} = G_1/A$ for protons. The values of G_1 and G_2 are taken as 19.60 and 15.70, respectively. In order to take into account, the weakened pairing effect in odd-mass systems due to the Pauli blocking effect, the values of G_{M_π} taken in refs. [19, 22] are reduced by a factor of 0.90 in the present calculations. G_{Q} is the quadrupole pairing strength which is taken as proportional to $\mathrm{G_M}$, and the proportionality constant in the present calculations is taken as 0.24. The strength of quadrupole–quadrupole interaction is denoted by χ, and its value is obtained by the self-consistent procedure from the value of deformation parameter $\in_2$ [27, 28].

The diagonalization of the Hamiltonian $\hat{H}$ in the model space of Eq. (2) yields the weights $f^I_{\kappa K}$ in Eq. (1) which further leads to the eigenvalue equation

$$\sum_{\kappa'}(H^I_{\kappa\kappa'} - EN^I_{\kappa\kappa'})f^I_{\kappa'} = 0, \tag{4}$$

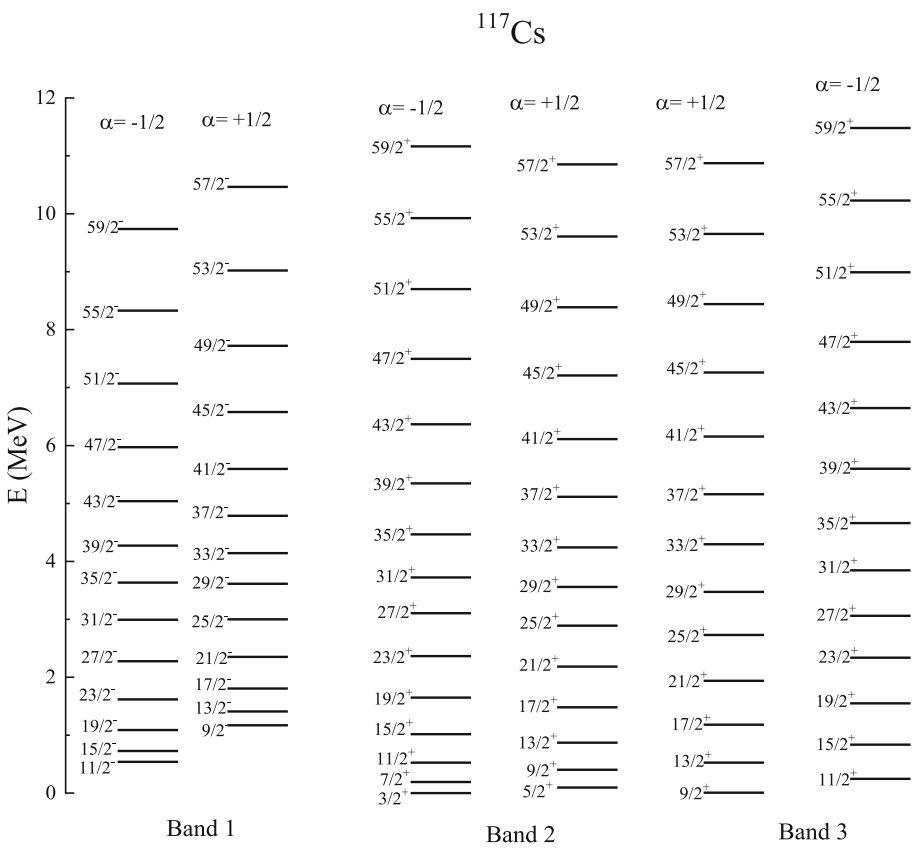

Fig. 4 Theoretical level scheme of ^{117}Cs

where

$$H^I_{\kappa\kappa'} = \left\langle \phi_\kappa | \hat{H} \hat{P}^I_{KK'} | \phi_{\kappa'} \right\rangle \text{ and } N^I_{\kappa\kappa'} = \left\langle \phi_\kappa | \hat{P}^I_{KK'} | \phi_{\kappa'} \right\rangle, \tag{5}$$

are Hamiltonian and norm overlaps, respectively.

The diagonal elements of Eq. (5) give the energies $E_\kappa(I)$ which are called rotational energies of each band of the band diagram [31]. These energies are given by

$$E_\kappa(I) = \frac{\left\langle \phi_\kappa | \hat{H} \hat{P}^I_{KK} | \phi_\kappa \right\rangle}{\left\langle \phi_\kappa | \hat{P}^I_{KK} | \phi_\kappa \right\rangle} = \frac{H^I_{\kappa\kappa}}{N^I_{\kappa\kappa}} \tag{6}$$

By analyzing the band diagram, one can predict the global behavior of various bands. The final results that can be compared with experimental data are obtained from the diagonalization of the Hamiltonian of Eq. (3).

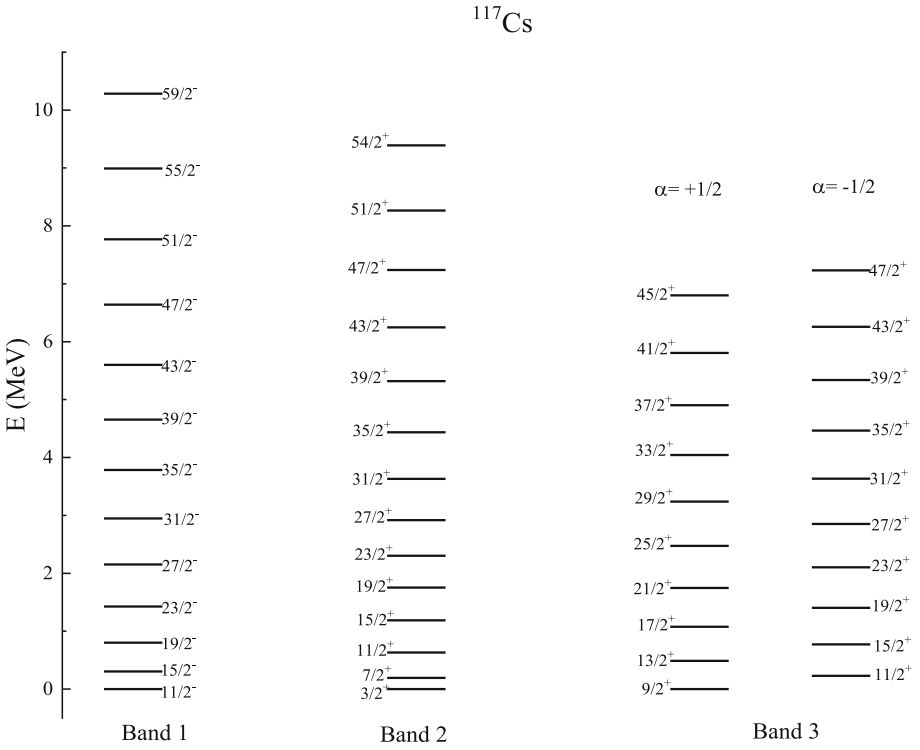

Fig. 5 Experimental level scheme of ^{117}Cs. The experimental level energies are taken from Ref. [6]

3 Results and discussion

From the available experimental data, it is found that very neutron-deficient $A \sim 120$, $Z = 55$ Cesium isotopes are well deformed with a value of quadrupole deformation $\varepsilon_2 \approx 0.25$. We have performed the PSM calculations for neutron-deficient odd-mass cesium isotopes with neutron number from 62 to 66. In the PSM, one first determines a deformed basis for a calculation to start with. The deformation parameters employed for generating the deformed basis in these calculations are listed in Table 1. These deformation parameters are nearly the same as suggested by Moller and Nix [32] and Routhian surface calculations [1, 6]. The positive and negative parity energy states are obtained by diagonalization of Hamiltonian (3) in the projected basis (2). The following subsections present the discussion on calculated energy levels of the yrast and some side bands which have been detected by experiments for odd proton $^{117-121}$Cs isotopes. The states up to spin $I = 59/2$ of each band are discussed and compared with the available experimental data.

3.1 Discussion of results on ^{117}Cs

The level scheme of ^{117}Cs has been studied by Smith et al. [6], and three bands have been obtained which are labeled as Band 1, Band 2 and Band 3. Band 1 is the negative parity band, and only one signature of Band 1 is observed. Band 1 is assigned the configuration $\pi(h_{11/2})[550]1/2^-$ orbital. Band 2 and Band 3 are positive parity bands and have been tentatively assigned the configurations $\pi(g_{7/2}/d_{5/2})[422]3/2^+$ and $\pi(g_{9/2})[404]9/2^+$ orbitals,

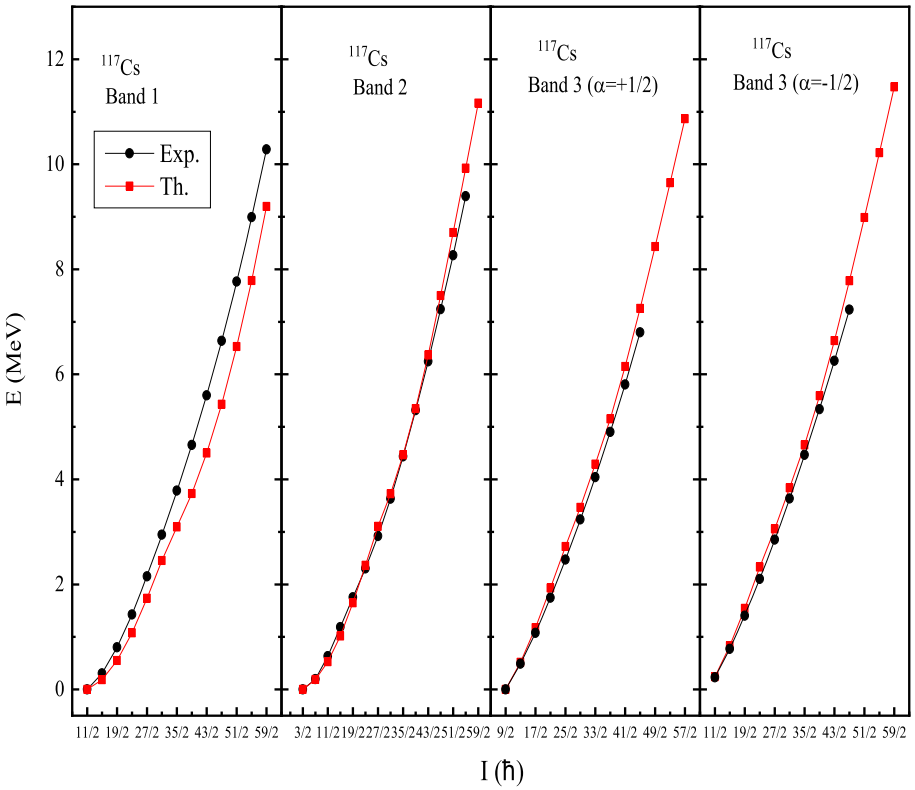

Fig. 6 Comparison of different calculated bands with experimental data with band head energy set equal to experimental band head energy in ^{117}Cs

respectively. The PSM calculations for ^{117}Cs have been performed by taking $\varepsilon_2 = 0.257$ and $\varepsilon_4 = -0.035$. For these deformation values, the $\pi(h_{11/2})[550]1/2^-$, $\pi(h_{11/2})[541]3/2^-$, $\pi(d_{5/2})[420]1/2^+$, $\pi(g_{7/2})[422]3/2^+$ and $\pi(g_{9/2})[404]9/2^+$ orbitals for protons lie near the Fermi surface. Thus, the bands based on these configurations are likely to be observed.

In Fig. 1, the low-lying bands in the form of band diagrams are presented for ^{117}Cs. The bands displayed in Figs. 1, 2, 3 have a definite value of quantum number K. The bands which lie close in energy have higher probability of mixing as compared to the bands which are well separated from each other. Thus, quantum number K is not conserved completely, but some degree of non-axiality may arise in the present calculations due to the mixing of bands with different configurations. The high-spin states of these bands will have more degree of intermixing of K quantum number due to the rotation of the nucleus.

From Fig. 1a, which displays band diagram for positive parity bands, it is seen that up to spin 7/2ħ, $\pi(g_{7/2})[422]3/2^+$ band is lowest in energy. Thus, the observed $\alpha = -1/2$ signature of Band 2 of Ref. [6] arises from $\pi(g_{7/2})[422]3/2^+$ configuration. The other $\alpha = +1/2$ signature partner of this band is not known experimentally, but the present calculation predicts its energy states as the superposition of $\pi(g_{7/2})[422]3/2^+$ and $\pi(d_{5/2})[420]1/2^+$ bands. Above spin 29/2ħ, these bands are crossed by the 3-qp bands. Thus, Band 2 of Ref. [6] is predicted as the ground state band. Second positive parity band labeled Band 3 of Ref. [6] has been assigned the configuration $\pi(g_{9/2})[404]9/2^+$ with band head at $9/2^+$. From Fig. 1a,

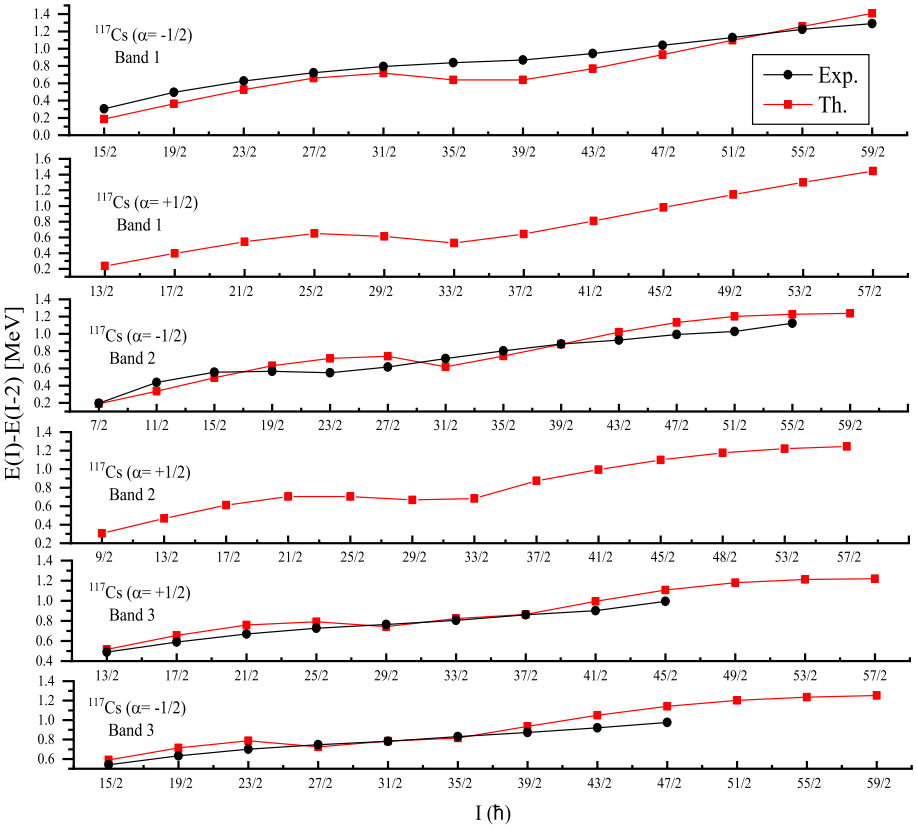

Fig. 7 Transition energy $E(I)$-$E(I\text{-}2)$ (in MeV) versus angular momentum I plots for ^{117}Cs

it is observed that $\pi(g_{9/2})[404]9/2^+$ band with $K = 9/2$ is lowest between spins 7/2 to 29/2 ħ. So, in agreement with experiment $\pi(g_{9/2})[404]9/2^+$ configuration is lowest in energy up to spin 29/2 ħ and above it, this band arises from superposition of 3-qp bands. The relative band head energy of this band is not yet known experimentally, but the present calculation predicts its relative band head energy at 6.9 keV with respect to predicted ground state Band 2.

Now coming to Fig. 1b, displaying band diagram for negative parity bands, it is seen that $\pi(h_{11/2})[550]1/2^-$, $\pi(h_{11/2})[541]3/2^-$ bands are lowest in energy among all negative parity bands. Experimentally this band is assigned the configuration $\pi(h_{11/2})[550]1/2^-$. This band is yrast band among the negative parity bands, and only one signature of this band is observed. The observed $\alpha = -1/2$ signature of Band 1 arises from $\pi(h_{11/2})[550]1/2^-$ configuration which is in agreement with experimental data. The signature partner of this band is not known experimentally, but the present calculation predicts signature partner of this band with $\alpha = +1/2$ as superposition of $\pi(h_{11/2})[550]1/2^-$ and $\pi(h_{11/2})[541]3/2^-$ bands. After spin $31/2^-$, $\pi(h_{11/2})[550]1/2^-$ and $\pi(h_{11/2})[541]3/2^-$ bands are crossed by 3-qp bands. The present calculation has also predicted relative band head energy of Band 1 as 541 keV with respect to band head energy of positive parity Band 2. The entire calculated level scheme for ^{117}Cs is presented in Fig. 4. This scheme should be compared to the experimental level scheme given in Fig. 5 of Ref. [6]. For completeness, the experimental levels of the same figure are plotted in Fig. 5 of this paper.

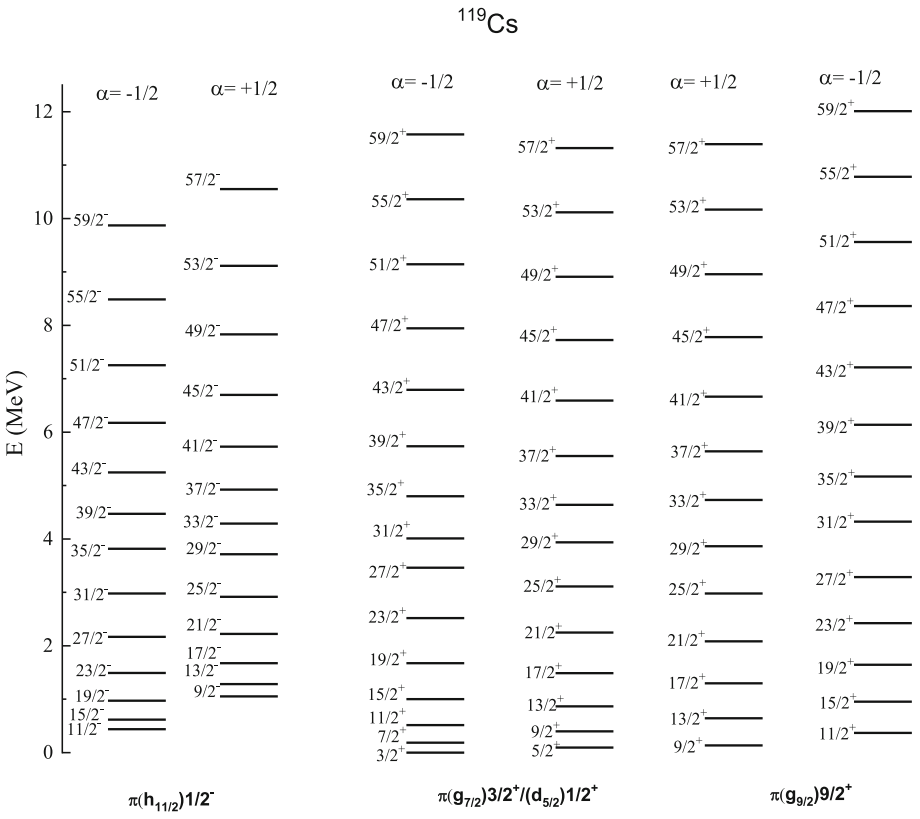

Fig. 8 Theoretical level scheme of ^{119}Cs

The calculated levels of different bands are compared with the experimental data by setting calculated band head energy equal to experimental band head energy in Fig. 6. From this figure, it is seen that for positive parity bands, the calculated energy states reproduce the experimental data qualitatively. However, for negative parity band the low-lying spin states show reasonable agreement with the experimental data. The transition energies $E(I)$–$E(I\text{-}2)$ (in MeV) are compared with the experimental data in Fig. 7. This figure reveals that the theoretical transition energies are in reasonable agreement with the experimental data.

3.2 Discussion of results on ^{119}Cs

The level scheme of ^{119}Cs has been extended to high spins by Liden et al. [1]. In this nucleus, one negative parity and one positive parity bands have been observed up to spins $35/2^-$ and $25/2^+$, respectively. The negative parity band has been assigned the configuration $\pi(h_{11/2})[550]1/2^-$ with $\alpha = -1/2$ and positive parity band has been assigned configuration $\pi(g_{9/2})[404]9/2^+$ with $\alpha = +1/2$ and $-1/2$. The PSM calculations are performed by taking $\varepsilon_2 = 0.250$ and $\varepsilon_4 = -0.035$ for all the bands. For these deformation values, the $\pi(h_{11/2})[550]1/2^-$, $\pi(h_{11/2})[541]3/2^-$, $\pi(d_{5/2})[420]1/2^+$, $\pi(g_{7/2})[422]3/2^+$ and $\pi(g_{9/2})[404]9/2^+$, orbitals for protons lie near the Fermi surface. Thus, the bands based on these configurations are likely to be observed. The band diagrams of significant bands are

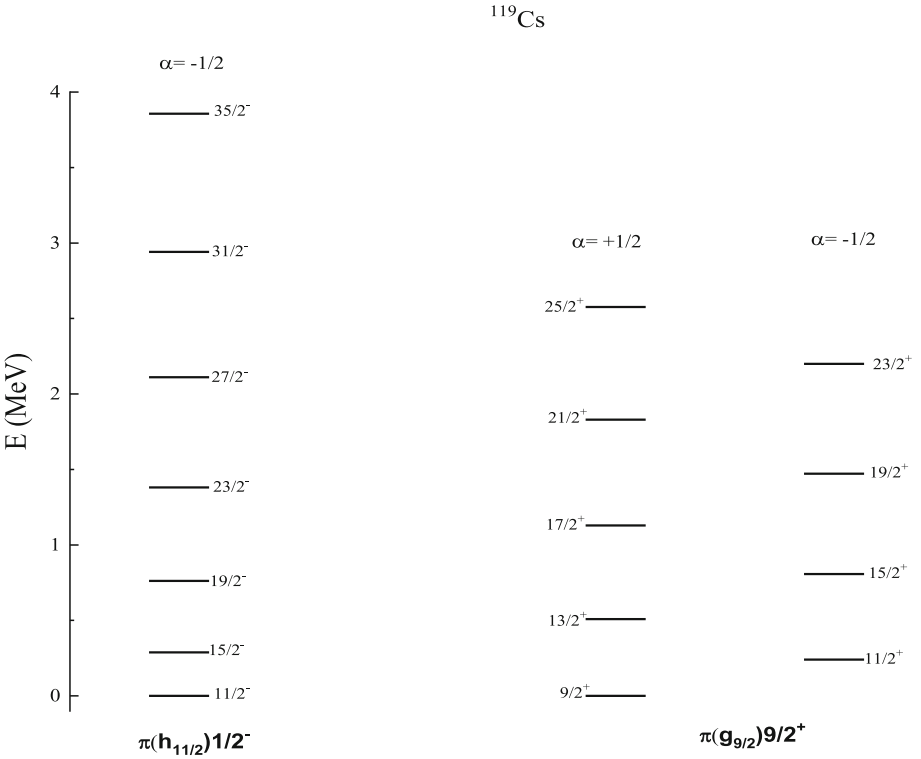

Fig. 9 Experimental level scheme of ^{119}Cs. The level energies are taken from Ref. [1]

presented in Fig. 2. From Fig. 2a, displaying band diagram for positive parity bands, it is observed that as in case of ^{117}Cs, $\pi(g_{9/2})[404]9/2^+$ band is lowest in energy between spins $9/2^+$ and $29/2^+$. Experimentally, this band is assigned the configuration $\pi(g_{9/2})[404]9/2^+$ which agrees with PSM calculations. In case of ^{117}Cs, one more $\pi(g_{7/2}/d_{5/2})[422]$ band is observed, but in case of ^{119}Cs, this band is not identified experimentally. The present calculation predicts one more positive parity band with the same configuration, i.e., $\pi(g_{7/2})[422]3/2^+$ with superposition of $\pi(d_{5/2})[420]1/2^+$ configuration as in case of ^{117}Cs. The PSM calculation predicts $\pi(g_{7/2}/d_{5/2})$ band as the ground state band and relative band head energy of $\pi(g_{9/2})[404]9/2^+$ band with respect to it is predicted as 136 keV which is yet not known experimentally. Now, in case of negative parity bands, one band is observed up to spin $35/2^-$ with E2 transitions that has been assigned configuration $\pi(h_{11/2})[550]1/2^-$. From Fig. 2b, displaying band diagram for negative parity bands, it can be seen that the states of observed negative parity band up to spin $35/2^-$ arise from $\pi(h_{11/2})[550]1/2^-$ configuration. After spin $35/2^-$, this band is crossed by 3-qp bands. The signature partner of this band is not known experimentally, but present calculation predicts signature partner of this band with $\alpha = +1/2$. A careful look at the bands presented in Fig. 2b shows that the angular momentum states of this band may have some admixture of $\pi(h_{11/2})[541]3/2^-$ band as seen in ^{117}Cs. We have also predicted relative band head energy of this band with respect to band head energy of predicted g-band $\pi(g_{7/2}/d_{5/2})$ as 437 keV. The entire calculated level scheme for ^{119}Cs is presented in Fig. 8. This scheme should be compared to the experimental level scheme given in Ref. [1]. For completeness, the experimental levels of the same figure are plotted in Fig. 9 of this paper.

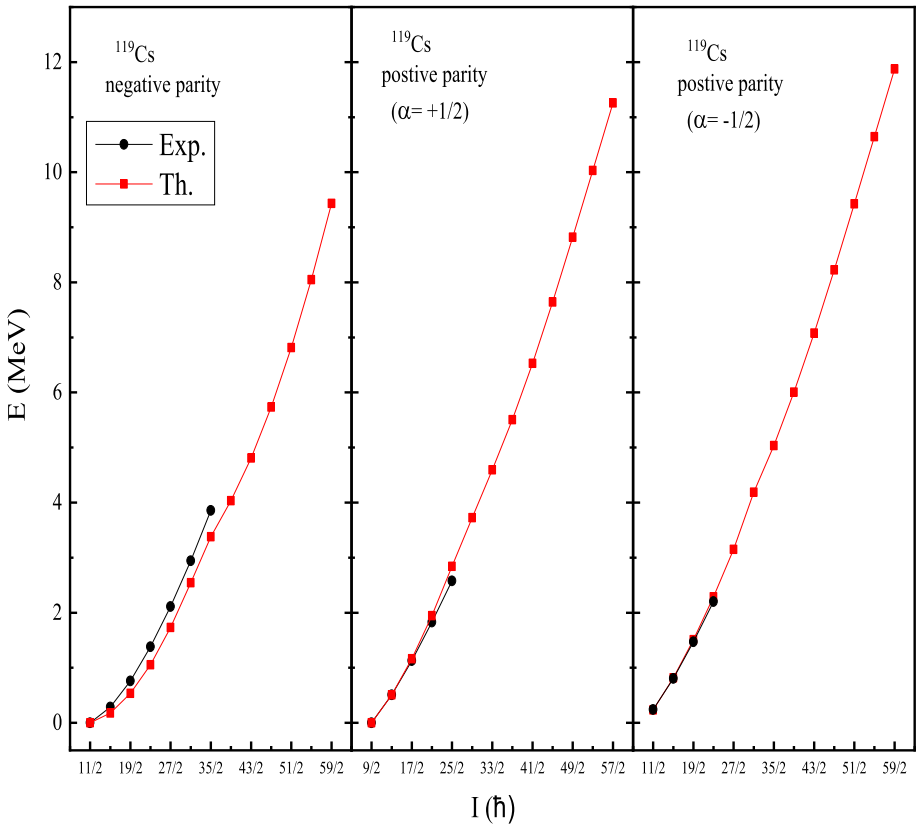

Fig. 10 Comparison of different calculated bands with experimental data with band head energy set equal to experimental band head energy in ^{119}Cs

The calculated levels of various bands are compared with the experimental data by setting calculated band head energy equal to experimental band head energy in Fig. 10. The calculated energies of various bands are seen to reproduce the experimental energies of bands nicely. The calculated transition energies E(I)-E(I-2) (in MeV) of various bands are compared with the experimental data in Fig. 11. This figure shows the reasonable agreement between calculated and available experimental energies.

3.3 Discussion of results on ^{121}Cs

The level scheme of ^{121}Cs has been extended to high spins by Liden et al. [1] and Moon et al. [9]. Moon et al. [9] have observed the negative parity band built on $1h_{11/2}$ band head and predicted its unfavored branch up to spin $I = 37/2^-$. Cranked shell model calculations have assigned $\pi(h_{11/2})[550]1/2^-$ configuration to this band. The experimental data of Ref. [10] present two positive parity and four negative parity bands for this nucleus. The positive parity bands labeled B and C have been assigned the configurations $\pi(g_{7/2})[422]3/2^+$ and $\pi(g_{9/2})[404]9/2^+$ proton bands, respectively. The PSM calculations are performed by taking $\varepsilon_2 = 0.257$ and $\varepsilon_4 = -0.045$ for all the bands. For these deformation values, the $\pi(h_{11/2})[550]1/2^-$, $\pi(h_{11/2})[541]3/2^-$, $\pi(d_{5/2})[420]1/2^+$, $\pi(g_{7/2})[422]3/2^+$ and

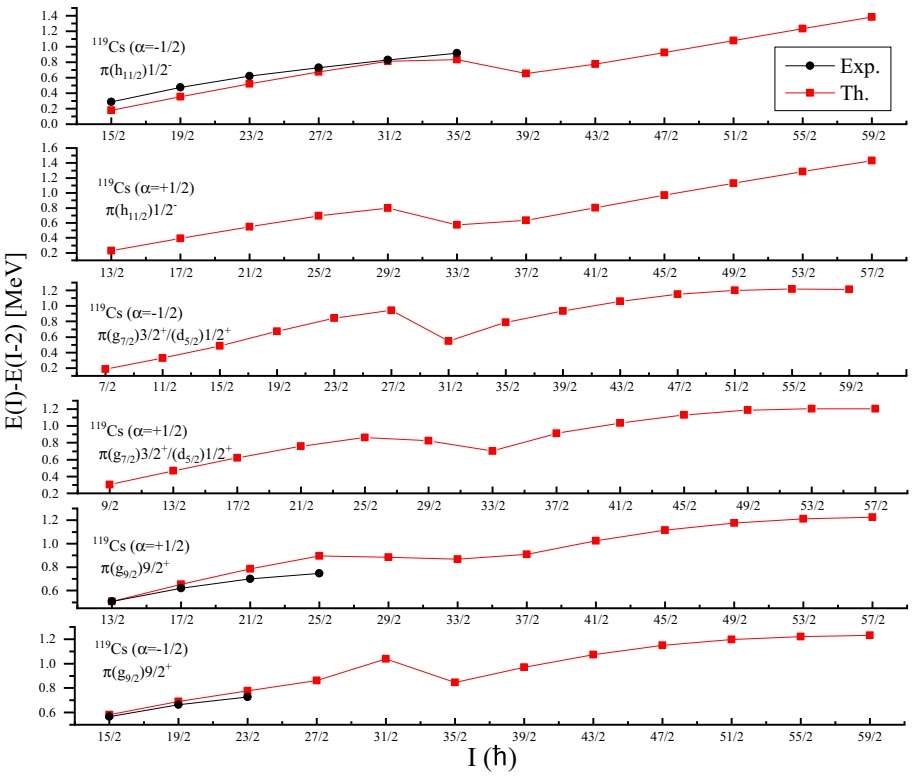

Fig. 11 Transition energy $E(I)$-$E(I\text{-}2)$ (in MeV) versus angular momentum I plots for ^{119}Cs

$\pi(g_{9/2})[404]9/2^+$ orbitals for protons lie near the Fermi surface. Thus, the bands based on these configurations are likely to be observed. The band diagrams of significant bands are presented in Fig. 3.

In case of positive parity bands of Ref. [10], Band B is ground band and assigned the configuration $\pi(g_{7/2})[422]3/2^+$ with band head spin $3/2^+$. From Fig. 3a, displaying band diagram of positive parity bands, it is seen that up to spin 7/2 ħ, $\pi(d_{5/2})[420]1/2^+$ and $\pi(g_{7/2})[422]3/2^+$ bands are lowest in energy. Thus, the observed energy states of Band B arise from $\pi(g_{7/2})[422]3/2^+$ configuration. The other signature partner of this band is not known experimentally, but the present calculation predicts its energy states arising from the superposition of $\pi(g_{7/2})[422]3/2^+$ and $\pi(d_{5/2})[420]1/2^+$ bands. Above spin 29/2 ħ, these bands are crossed by the 3-qp bands. Second positive parity band labeled Band C of Ref. [10] has been assigned the configuration $\pi(g_{9/2})[404]9/2^+$ with band head at spin $9/2^+$. Experimentally, the band head of this band is observed at an energy of 68.5 keV with respect to band head energy of Band B. PSM calculation predicts the band head of this band at an energy of 5.8 keV. From Fig. 3a displaying band diagram for positive parity bands, it is observed that $\pi(g_{9/2})[404]9/2^+$ is lowest in energy between spins $7/2^+$ to $37/2^+$. So, in agreement with experiment $\pi(g_{9/2})[404]9/2^+$ configuration is lowest in energy between spins $7/2^+$ to $37/2^+$ and above spin $37/2^+$, this band arises from superposition of energies of 3-qp bands. From Fig. 3b, displaying band diagram for negative parity bands, it is observed from this figure that the negative parity bands show staggering. The $\pi(h_{11/2})[550]1/2^-$ band shows large signature

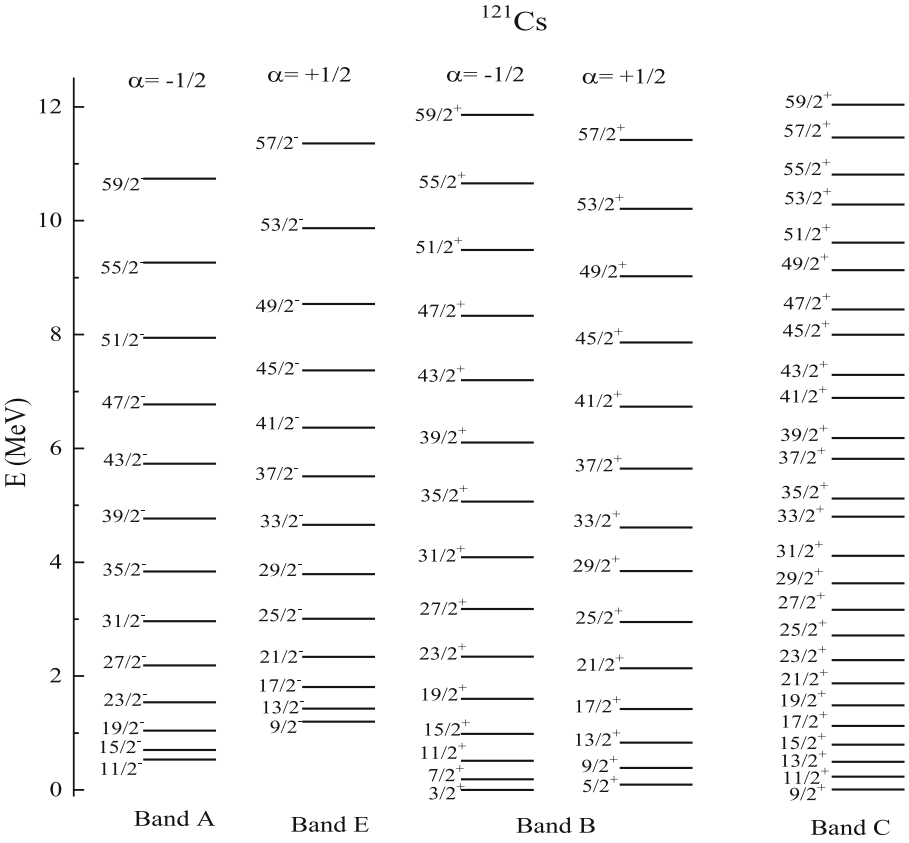

Fig. 12 Theoretical level scheme of ^{121}Cs

splitting for low K components as compared to $\pi(h_{11/2})[541]3/2^-$ band. The experimental data show that yrast negative parity band is built on $1h_{11/2}$ band head. From band diagram, it is observed that $K = 1/2$ and $K = -3/2$ $1\pi(h_{11/2})$ bands are lowest up to spin 27/2 ħ. Thus, the negative parity yrast band is having some contribution from $K = 3/2$ component of $1\pi(h_{11/2})$ band also. The present calculation predicts that the experimentally observed decoupled band based on $1\pi h_{11/2}$ labeled Band A in Ref. [10] arises from favored states of $\pi(h_{11/2})[550]1/2^-$ band, whereas experimentally observed Band E of Ref. [10] arises from superposition of unfavored states of $\pi(h_{11/2})[550]1/2^-$ and $\pi(h_{11/2})[541]3/2^-$ bands. Thus, we predict Band E as unfavored branch of Band A. Above spin 27/2 ħ, these bands are crossed by 3-qp bands. In the present calculations, we have predicted relative band head energy of Band A with respect to band head energy of g-band that is Band B as 533 keV that is not yet known experimentally. The entire calculated level scheme for ^{121}Cs is presented in Fig. 12. This scheme should be compared to the experimental level scheme given in Ref. [10]. For completeness, some experimental bands of same figure [10] are plotted in Fig. 13 of this paper.

The calculated levels of various bands are compared with the experimental data by setting calculated band head energy equal to experimental band head energy in Fig. 14. This figure shows that the calculated energy reproduces the experimental data qualitatively. Figure 15 presents the comparison of calculated and experimental transition energies E(I)-E(I-2) (in

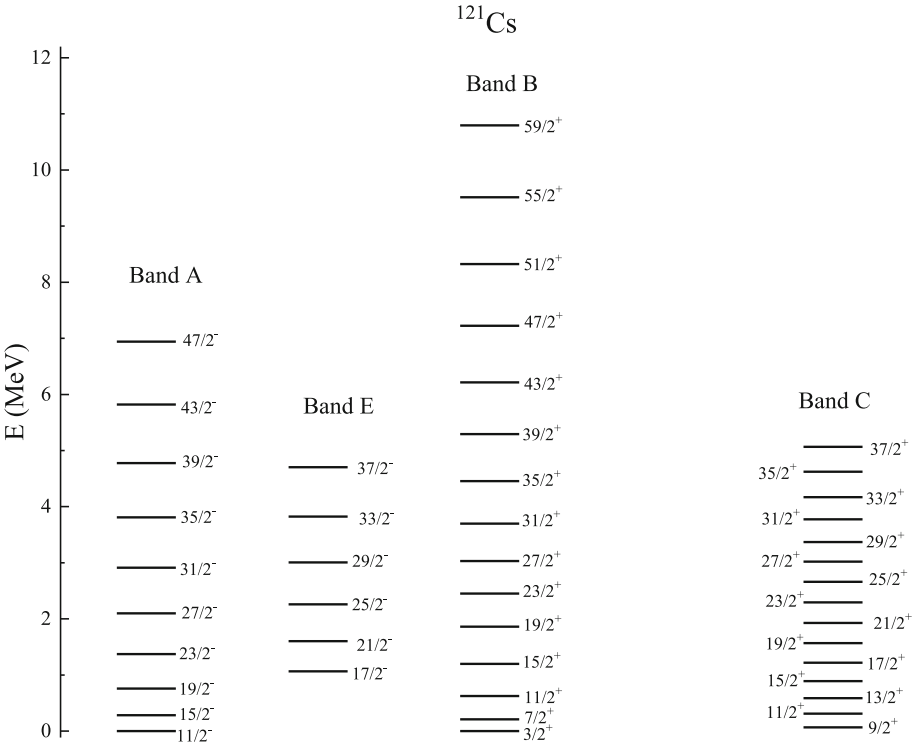

Fig. 13 Experimental level scheme of ^{121}Cs. The experimental level energies are taken from Ref. [10]

MeV) of positive parity bands. From this figure, it is observed that the calculated energies are in reasonable agreement with the experimental data.

4 Analysis of signature splitting in ^{117,119,121}Cs

The signature splitting in odd-mass nuclei was described by Sun and Hara [11] by using PSM approach. Signature quantum number appears in a deformed intrinsic system which is related to the invariance of a system with quadrupole deformation under rotation of 180° around a principal axis. For an odd-mass nucleus, it can take two different values. The signature quantum number for a state of spin I for an odd- mass nucleus is assigned as $\alpha_I = \frac{1}{2}(-1)^{I-1/2.}$ The sequence of levels in a rotational band differing in spin by 1ħ can be divided into two branches, each consisting of levels differing in spin by 2ħ and classified by the signature quantum number $\alpha_I = \pm\frac{1}{2}$, respectively. Experimentally, for some bands an energy splitting for the two branches is observed. The spin I states that satisfy I-j = even, where j is the total angular momentum of the corresponding single-particle state, form the energetically favored branch of the band. According to this rule, the favored branch of $\pi(h_{11/2})[550]1/2^-$ (j= 11/2) band consists of the spin levels I= 3/2, 7/2, 11/2, 15/2, … The unfavored band consists of I= 1/2, 5/2, 9/2, … As only favored band is known experimentally, we have predicted unfavored branch with signature quantum number α =+1/2 for ^{117,119}Cs.

In Figs. 1, 2, and 3, band diagrams of $^{117-121}$Cs are plotted. From these figures, it is seen that the negative parity bands $\pi(h_{11/2})[550]1/2^-$, K = 1/2 and $\pi(h_{11/2})[541]3/2^-$, K = 3/2 have

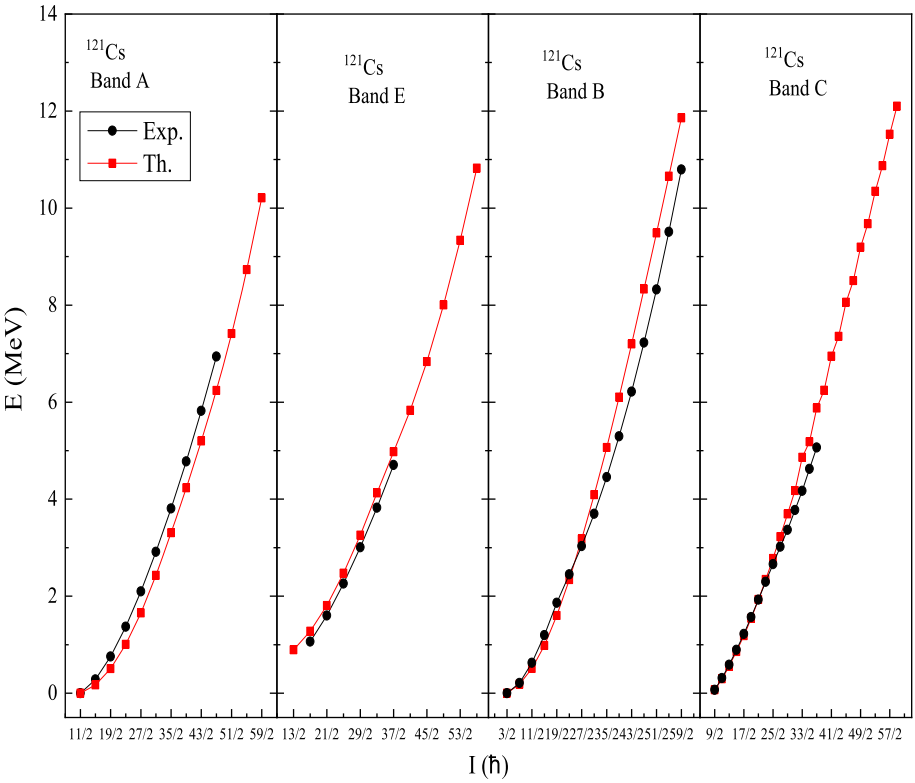

Fig. 14 Comparison of different calculated bands with experimental data with band head energy set equal to experimental band head energy in ^{121}Cs

zigzag behavior. However, it is observed that the negative parity band $\pi(h_{11/2})[550]1/2^-$, $K = 1/2$ has more pronounced zigzag behavior. These irregularities are attributed to the decoupling effect [33] which is usually seen in rotational bands with a high j and low K state (e.g., $K = 1/2$ or $K = 3/2$) as the main configuration. The zigzag behavior of these bands shows that they have two signature partners and the signature partner with $\alpha = -1/2$ is pushed down in as compared to its counterpart. In all these nuclei because of low-lying components of proton $1h_{11/2}$ orbital, the negative parity bands show staggering. In Fig. 16, the $E(I)$-$E(I-1)$ (in MeV) is plotted as function of spin. From this figure, it is clear that the negative parity bands in all the three nuclei show staggering. The amplitude of the staggering decreases at the spin around which 1-qp bands are crossed by 3-qp bands. As the experimental data for unfavored band with $\alpha = +1/2$ are not known for ^{117,119}Cs, so it is not possible to make any comment. However, in case of ^{121}Cs, the experimental data are available up to spin 39/2 ħ which is reproduced by the present calculations.

Now coming to band diagrams of positive parity bands displayed in Figs. 1, 2, and 3, it is observed that $\pi(g_{7/2})[422]3/2^+$, $K = 3/2$ band shows less zigzag pattern as compared to negative parity bands in all the nuclei. The other positive parity bands are showing smooth behaviors. From Fig. 16, it is clear that positive parity band labeled Band 2, $\pi(g_{7/2})/(d_{5/2})$ or B predict signature splitting with less amplitude as compared to negative parity bands. However, 1-qp $\pi(g_{9/2})[404]9/2^+$, $K = 9/2$ band shows no signature splitting up to band crossing region both experimentally and theoretically.

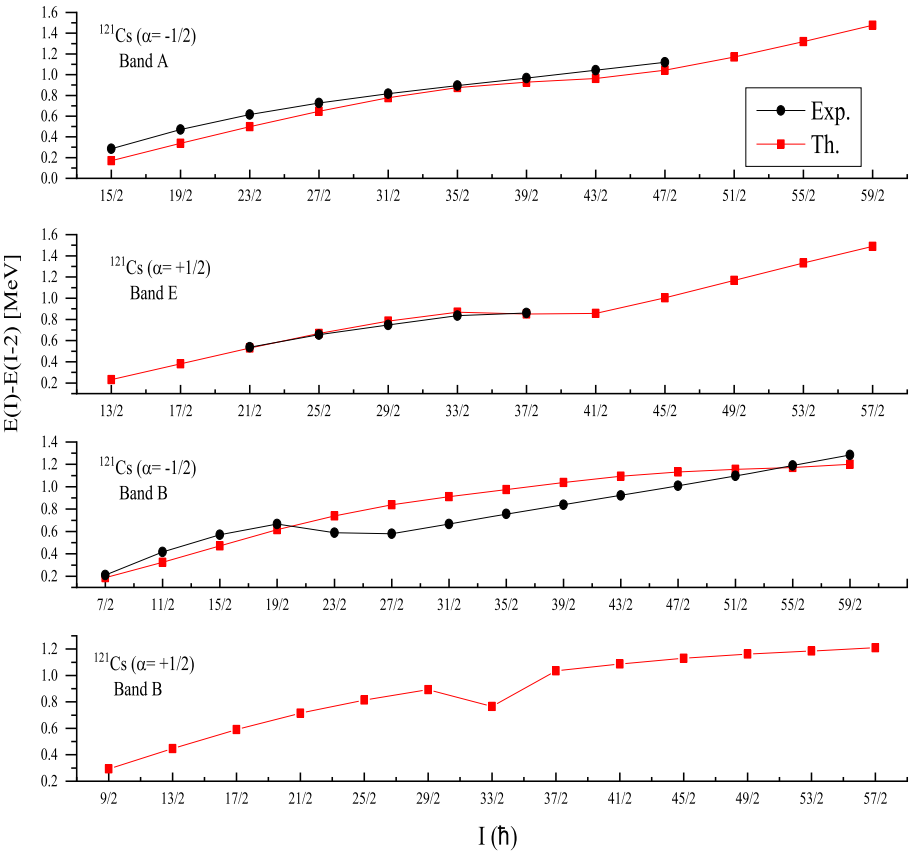

Fig. 15 Transition energy $E(I)$-$E(I\text{-}2)$ (in MeV) versus angular momentum I plots for ^{121}Cs

5 Summary

The neutron-deficient cesium isotopes with $N = 62$–66 are studied by using PSM approach by taking same set of Nilsson parameters as employed in earlier PSM calculations in $A \sim 120$ mass region [19–22]. The experimentally observed bands are investigated and relative energies of some bands are predicted. In case of ^{117}Cs all the bands are obtained and their configurations are consistent with the experimental data. The relative band head energy of bands is not known experimentally but the present calculations have predicted the relative band head energies of bands with respect to $\pi(g_{7/2})[422]3/2^+$ band. In addition, the signature partner band of negative and positive parity bands is also predicted.

In case of ^{119}Cs, the level energies of known bands are reproduced qualitatively and signature partner of negative parity band is predicted. For positive parity bands, one new band with configuration $\pi(g_{7/2}/d_{5/2})$ is predicted and relative band head energies of all the bands with respect to this band are also predicted.

The present calculation reproduces the level energies of the experimental bands in ^{121}Cs and predicted the unknown signature partner band of positive parity band. The experimentally observed signature splitting in negative parity bands is reproduced by the present calculation qualitatively. Besides this, it is observed that the signature splitting is more pronounced in

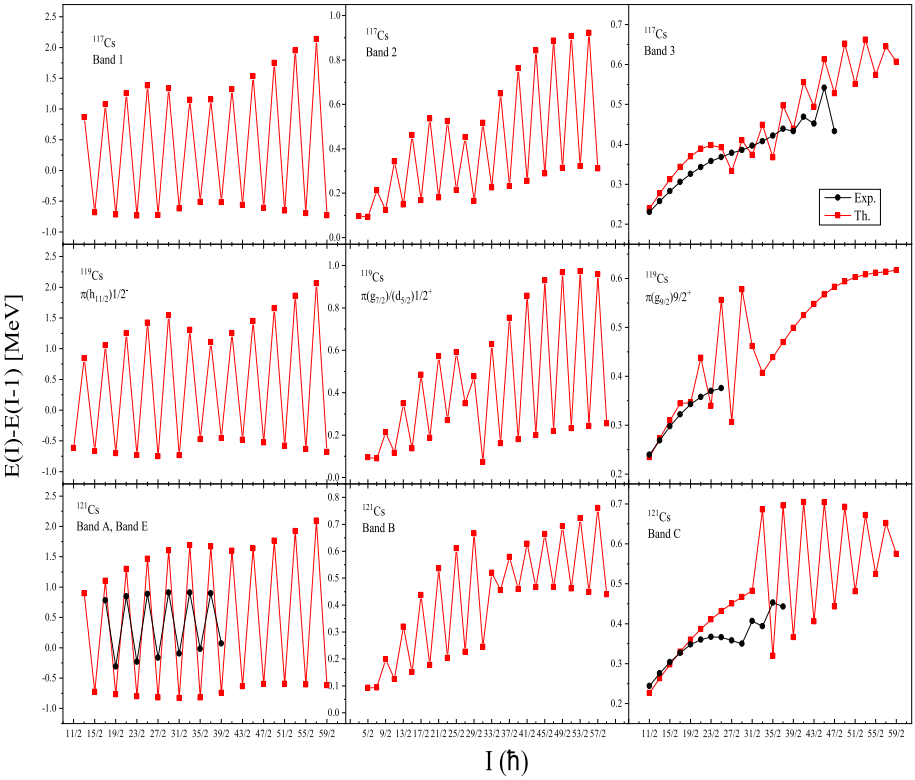

Fig. 16 The transition energy of ^{117,119,121}Cs. The energy difference $E(I)$-$E(I\text{-}1)$ (in MeV) is compared between theory and experiment. The first column is for negative parity bands in ^{117,119,121}Cs; the second and third columns are for positive parity bands in ^{117,119,121}Cs, respectively

negative parity bands as compared to positive parity ground state bands in these nuclei due to the occupation of low K components of high j orbitals. The predicted relative band head energies and bands may trigger experimentalists to plan new experiments to study these neutron-deficient Cs isotopes in future.

References

1. F. Liden et al., Nucl. Phys. A **550**, 365 (1992)
2. J.R. Hughes, D.B. Fossan, D.R. LaFose, Y. Liang, P. Vaska, M.P. Waring, J.Y. Zhang, Phys. Rev. C **45**, 2177 (1992)
3. J.R. Hughes, D.B. Fossan, D.R. LaFosse, Y. Liang, P. Vaska, M.P. Waring, Phys. Rev. C **44**, 2390 (1991)
4. Y. Liang, R. Ma, E.S. Paul, N. Xu, D.B. Fossan, R. Wyss, Phys. Rev. C **42**, 890 (1990)
5. L. Hildingsson, W. Klamra, T. Lindblad, F. Liden, Y. Liang, R. Ma, E.S. Paul, N. Xu, D.B. Fossan, J. Gascon, Z. Phys. A **340**, 29 (1991)
6. J.F. Smith et al., Phys. Rev. C **63**, 024319 (2001)
7. X. Sun et al., Phys. Rev. C **51**, 2803 (1995)
8. U. Garg, T.P. Sjoreen, D.B. Fossan, Phys. Rev. C **19**, 217 (1979)
9. C.B. Moon, T. Komatsubara, K. Furuno, J. Korean Phys. Soc. **38**, 8 (2001)
10. S. Ohya, Nucl. Data Sheets **111**, 1619 (2010)
11. K. Hara, Y. Sun, Nucl. Phys. A **537**, 77 (1992)

12. A. Ibáñez-Sandoval, V. Velázquez, A. Galindo-Uribarri, P.O. Hess, Y. Sun, Phys. Rev. C **83**, 034308 (2011)
13. Y. Sun, M. Guidry, Phys. Rev. C **52**, R2844 (1995)
14. Y. Sun, J.Y. Zhang, M. Guidry, Phys. Rev. Lett. **78**, 2321 (1997)
15. Y. Sun, J.Y. Zhang, M. Guidry, C.L. Wu, Phys. Rev. Lett. **83**, 686 (1999)
16. V. Velázquez, J. Hirsch, Y. Sun, M. Guidry, Nucl. Phys. A **653**, 335 (1999)
17. V. Velázquez, J. Hirsch, Y. Sun, Nucl. Phys. A **686**, 129 (2001)
18. R. Palit, J.A. Sheikh, Y. Sun, H.C. Jain, Phys. Rev. C **67**, 014321 (2003)
19. R. Devi, B.D. Sehgal, S.K. Khosa, J.A. Sheikh, Phys. Rev. C **72**, 064304 (2005)
20. B.D. Sehgal, R. Devi, S.K. Khosa, J. Phys. G **32**, 1211 (2006)
21. R. Kumar, R. Devi, S.K. Khosa, Phys. Scr. **80**, 045201 (2009)
22. R. Devi, B.D. Sehgal, S.K. Khosa, Pramana-J. Phys. **67**, 467 (2006)
23. S. Verma, P.A. Dar, R. Devi, Phys. Rev. C **77**, 024308 (2008)
24. Y.C. Yang, Y. Sun, S.J. Zhu, M. Guidry, C.L. Wu, J. Phys. G **37**, 085110 (2010)
25. F. Al-Kudair, G.L. Long, Y. Sun, Phys. Rev. C **79**, 034320 (2009)
26. Y. Sun, Y.C. Yang, H.L. Liu, K. Kaneko, M. Hasegawa, T. Mizusaki, Phys. Rev. C **80**, 05430 (2009)
27. Y. Sun, Phys. Scr. **91**, 043005 (2016)
28. K. Hara, Y. Sun, Int. J. Mod. Phys. E **4**, 637 (1995)
29. S.G. Nilsson, C.F. Tsang, A. Sobiczewski, Z. Szymanski, S. Wycech, Ch. Gustafson, I.L. Lamm, P. Moller, B. Nilsson, Nucl. Phys. A **131**, 1 (1969)
30. P. Ring, P. Schuck, *The Nuclear theory Many Body Problem* (Springer, New York, 1980)
31. K. Hara, Y. Sun, Nucl. Phys. A **529**, 445 (1991)
32. P. Möller, J.R. Nix, W.D. Myers, W.J. Swiatecki, At. Data Nucl. Data Tables **59**, 185 (1995)
33. Y. Sun, D.H. Feng, S.X. Wen, Phys. Rev. C **50**, 2351 (1994)